SCISPACE
formerly Typeset

Open access • Journal Article • DOI:10.1103/PHYSREVB.95.115438

Wigner crystallization in transition metal dichalcogenides: A new approach to correlation energy — Source link

Mohammad Zarenia, David Neilson, Bart Partoens, François M. Peeters

Institutions: University of Antwerp, University of Camerino

Published on: 29 Mar 2017 - Physical Review B (American Physical Society)

Topics: Wigner crystal, Fermi liquid theory, Quantum Monte Carlo, Fermi gas and Random phase approximation

Related papers:

- Correlation energy and spin polarization in the 2D electron gas.
- On the Interaction of Electrons in Metals
- k · p theory for two-dimensional transition metal dichalcogenide semiconductors
- Fermi polaron-polaritons in charge-tunable atomically thin semiconductors
- Theory of neutral and charged excitons in monolayer transition metal dichalcogenides

Share this paper:

View more about this paper here: https://typeset.io/papers/wigner-crystallization-in-transition-metal-dichalcogenides-a-wkpiu671zg

Wigner crystallization in transition metal dichalcogenides: A new approach to correlation energy

M. Zarenia,[1] D. Neilson,[2] B. Partoens,[1] and F. M. Peeters[1]

[1]*Department of Physics, University of Antwerp, Groenenborgerlaan 171, B-2020 Antwerpen, Belgium*

[2]*Dipartimento di Fisica, Università di Camerino, via Madonna delle Carceri 9, 62032 Camerino, Italy*

(Received 15 November 2016; revised manuscript received 20 February 2017; published 29 March 2017)

We introduce a new approach for the correlation energy of one- and two-valley two-dimensional electron gas (2DEG) systems. Our approach is based on an interpolation between two limits, a random phase approximation at high densities and a classical approach at low densities which gives excellent agreement with available Quantum Monte Carlo (QMC) calculations. The two-valley 2DEG model is introduced to describe the electron correlations in monolayer transition metal dichalcogenides (TMDs). We study the zero-temperature transition from a Fermi liquid to a quantum Wigner crystal phase in monolayer TMDs. Consistent with QMC, we find that electrons crystallize at $r_s = 31$ in one-valley 2DEG. For two valleys, we predict Wigner crystallization at $r_s = 30$, implying that valley degeneracy has little effect on the critical r_s, in contrast to an earlier claim.

DOI: 10.1103/PhysRevB.95.115438

I. INTRODUCTION

For a two-dimensional (2D) electron gas (2DEG) in a conventional semiconductor, quantum Wigner crystallization (WC), i.e., freezing of electrons induced by very strong electron-electron interactions [1], is predicted to occur only for extremely low electron densities ρ, corresponding to $r_s \gtrsim 31$, see Refs. [2–5]. Following Ref. [6] we define the parameter $r_s = 1/\sqrt{\pi\rho}a_B^*$ for both one- and two-valley systems. r_s measures the relative importance of the average electron-electron interaction energy to the Fermi energy. a_B^* is the effective Bohr radius.

The quantum WC at zero magnetic field has not yet been observed and remains an experimental challenge. Of the new 2D materials such as graphene and the semiconducting transition metal dichalcogenides (TMDs), e.g., MoS_2, WS_2, $MoSe_2$, WSe_2, WTe_2, etc. [7–9], graphene is always a weakly interacting system since r_s in a graphene monolayer is always less than unity independent of the density [10]. For this reason graphene is expected not to exhibit a WC transition [11]. In contrast, for TMD monolayers with quasiquadratic low energy dispersions, r_s is density dependent and becomes large for experimentally accessible densities. For example, at a density $\rho = 1 \times 10^{11}$ cm^{-2} in monolayer MoS_2 (see supplementary of Ref. [12]), one has $r_s \sim 30$. This makes monolayer TMDs a new class of candidates where the quantum WC may be experimentally observable.

At low densities, the correlations between the electrons due to the repulsive Coulomb interaction become sufficiently strong to drive the system from a liquid phase to the WC phase. The inversion symmetry breaking in 2D monolayer TMDs leads to a direct band gap located at the two inequivalent valleys at the K points (corners of the first Brillouin zone). With the additional valley index degree of freedom the electrons have significantly different correlation energies than electrons at the same density in a one-valley system.

The energy differences between the WC and liquid phases are very small and to get reliable predictions, extremely high accuracy such as offered by Quantum Monte Carlo (QMC) methods is required [2,3,6]. Reference [6] obtained the correlation energy for a two-valley 2DEG system using QMC calculations to describe the ground state energy of electrons confined in a Si metal-oxide-semiconductor field-effect transistor (MOSFET). They predicted that for two valleys the density for the WC transition shifts to a much lower density, $r_s \approx 45$. This would make the formation of the WC much more difficult as compared to the one-valley system. However, in the present work we challenge this result.

Apart from pinning the WC, disorder in monolayer TMDs is not expected to play an important role in the WC transition. For example, for a typical low temperature mobility value in a high quality sample of MoS_2 of 500 cm^2/(V.s), the corresponding disorder energy scale is only ∼5 meV [13], while the average Coulomb interaction energy exceeds 40 meV, even at a density as low as $\rho = 1 \times 10^{11}$ cm^{-2}. In the present work we neglect disorder.

There can be spin polarization in the TMDs at very low densities because of splitting of the spin bands by spin-orbit coupling (SOC). However, for densities near the WC transition in the one-valley system, spin polarization should have little effect on our quantitative conclusions and we neglect it. The reason is that by such low densities the spin-polarized and unpolarized pair correlation functions have become very similar [4]. In addition, the large semiconducting gap in TMDs means that we need only to consider the conduction band in which the SOC splitting $\Delta_{\rm SOC}^{\rm c}$ is much smaller than in the valence band. However, for lowest densities, $\Delta_{\rm SOC}^{\rm c}$ in the conduction band [14] can be significant on the scale of the Fermi energy, resulting in some spin polarization.

In our work we first discuss a density functional approach to describe the ground state energy for a nonuniform density distribution corresponding to a 2D hexagonal lattice. To obtain the correlation energy in monolayer TMDs, i.e., two-valley 2DEG system, we then introduce a new approach based on the random phase approximation (RPA) at high densities and a classical approach at low densities. We demonstrate that our results for the correlation energies are in very good agreement with QMC for both one-valley and two-valley 2DEG systems. We discuss our results for the WC and liquid ground state energy as a function of density in Sec. IV and present a summary and conclusions of the paper in Sec. V.

II. DENSITY FUNCTIONAL THEORY

We recall that in density functional theory the ground state energy functional $E[\rho]$ for a system of interacting electrons

 ©2017 American Physical Society

with density distribution $\rho(\boldsymbol{r})$ is written as the sum,

$$E[\rho] = K[\rho] + E_{\rm coul}[\rho] + E_{\rm x}[\rho] + E_{\rm c}[\rho], \quad (1)$$

where $K[\rho]$, $E_{\rm coul}[\rho]$, $E_{\rm x}[\rho]$, and $E_{\rm c}[\rho]$, respectively, denote the noninteracting kinetic energy, Hartree term, exchange, and correlation energy functionals of the density distribution. We will compare the ground state energy for the liquid of uniform density ρ_0 with the ground state energy of the WC with nonuniform density distribution $\rho(\boldsymbol{r})$ on a 2D hexagonal lattice.

Within the local-density approximation (LDA), approximate forms of the kinetic-energy and Hartree functionals expressed in terms of inhomogeneous density distributions are,

$$K[\rho] = \frac{1}{8}\int d^2\boldsymbol{r}\frac{\nabla\rho(\boldsymbol{r})\cdot\nabla\rho(\boldsymbol{r})}{\rho(\boldsymbol{r})} + \frac{\pi}{2g_v}\int d^2\boldsymbol{r}\rho(\boldsymbol{r})^2, \quad (2)$$

and

$$E_{\rm coul} = \frac{1}{2}\int {\rm d}^2\boldsymbol{r}\int {\rm d}^2r'\frac{[\rho(\boldsymbol{r})-\rho_0][\rho(\boldsymbol{r'})-\rho_0]}{|\boldsymbol{r}-\boldsymbol{r'}|}. \quad (3)$$

$g_v = 1,2$ distinguishes the one- and two-valley 2DEG systems.

We also define the functional forms of the exchange and correlation energies within LDA. LDA assumes that the exchange-correlation energy $\epsilon_{xc}(\rho)$ at a point $\boldsymbol{r}$ is equal to the exchange-correlation energy of a uniform electron gas with the same density as at the point $\boldsymbol{r}$. Thus we can write

$$E_{xc}[\rho(\boldsymbol{r})] = \int \rho(\boldsymbol{r})\epsilon_{xc}(\rho)d\boldsymbol{r}. \quad (4)$$

Using Eq. (4) we write

$$E_{\rm x}[\rho] = -\frac{4}{3}\sqrt{\frac{2}{\pi g_v}}\int d^2\boldsymbol{r}\rho(\boldsymbol{r})^{3/2}, \quad (5)$$

$$E_{\rm c}[\rho] = \int d^2\boldsymbol{r}\rho(\boldsymbol{r})\epsilon_c[\rho(\boldsymbol{r}),g_v], \quad (6)$$

where $\epsilon_c[\rho_0,g_v]$ is the correlation energy for a system of uniform density ρ_0. In the next section we introduce a new approach to obtain $\epsilon_c[\rho_0,g_v]$.

III. CORRELATION ENERGY

An exact expression for the exchange-correlation functional $E_{xc}[\rho]$ in terms of the coupling constant integral was given in Refs. [15,16],

$$E_{\rm xc}[\rho] = \int_0^1 d\alpha W_\alpha[\rho], \quad (7)$$

where $W_\alpha[\rho] = \langle\Psi^\alpha[\rho]|\hat{V}_{ee}|\Psi^\alpha[\rho]\rangle - E_{\rm coul}[\rho]$ is the potential energy functional excluding the Hartree contribution, for a fictitious system interacting via a Coulomb-like interaction $\hat{V}_{ee} = \sum_{i<j}|\mathbf{r}_i - \mathbf{r}_j|^{-1}$ that is scaled by a multiplicative coupling constant factor α. Ψ^α is the wave function that minimizes the expectation value $\langle K[\rho] + \alpha\hat{V}_{ee}\rangle$ for the fictive electron system with the kinetic-energy operator K and the interaction $\alpha\hat{V}_{ee}$ with the same ground-state density ρ as for the real system where the interaction is $\hat{V}_{ee}^{\alpha=1}$.

Since $W_\alpha[\rho]$ is expected to be a smooth function of α [17], Refs. [18–20] proposed an interpolation procedure for $W_\alpha[\rho]$, between the $\alpha = 0$ (weakly-interacting, high density limit) and $\alpha = \infty$ (strongly-interacting, low density limit),

$$W_\alpha[\rho] \simeq W_\infty + \frac{W_0 - W_\infty}{\sqrt{1+2X\alpha}}, \quad X = \frac{W_0'}{W_\infty - W_0} \quad (8)$$

where $W_0' = {\rm d}W_\alpha/{\rm d}\alpha|_{\alpha=0}$. The properties required for W_α have been extensively discussed in Refs. [18–20]: W_α should be a smooth function of α and should converge to $W_0 + W_0'\alpha$ and W_∞ in the limits $\alpha \to 0$ and $\alpha \to \infty$, respectively.

Substituting Eq. (8) into Eq. (7) and integrating, we obtain for the correlation energy,

$$E_{\rm xc}[\rho] = W_0 + (W_0 - W_\infty)\left[\frac{\sqrt{1+2X}-1}{X} - 1\right]. \quad (9)$$

Weakly-interacting regime. We employ RPA to obtain W_0 and W_0'. We recall that RPA is exact in the high-density limit [22]. Using RPA offers significant advantages over the approach of Ref. [19] which calculated W_0 for a 2DEG using the Fock integral with the (occupied) Kohn-Sham orbitals while W_0' was the second order coefficient in Görling-Levy perturbation theory [21]. In particular our RPA calculations of W_0 and W_0' can be readily generalized to finite temperatures and to nonparabolic energy dispersions.

There exist exact expressions for $W_0[\rho]$ and $W_0'[\rho]$ [22],

$$\begin{aligned} W_0[\rho] &= W_{\rm RPA}[\rho], \\ W_0'[\rho] &= W_{\rm RPA}'[\rho] + W_0^{(2)\prime}[\rho], \end{aligned} \quad (10)$$

where the RPA interaction energy $W_{\rm RPA}[\rho]$ and its derivative with respect to α, $W_{\rm RPA}'[\rho]$, are expressed as integrals along the imaginary frequency axis,

$$\begin{aligned} W_{\rm RPA}[\rho] &= \sum_{\boldsymbol{q}} v_q\left[-\frac{\hbar}{2\pi\rho}\int_0^\infty {\rm d}\omega\chi_0(\boldsymbol{q},i\omega) - 1\right], \\ W_{\rm RPA}'[\rho] &= -\frac{\hbar}{2\pi\rho}\sum_{\boldsymbol{q}} v_q\int_0^\infty {\rm d}\omega[{\rm d}\chi_\alpha(\boldsymbol{q},i\omega)/{\rm d}\alpha]_{\alpha=0}. \end{aligned} \quad (11)$$

$v_q = e^2/\kappa q$ is the Coulomb potential with κ the dielectric constant and $\chi_\alpha(\boldsymbol{q},i\omega)$ is the RPA density-density response function.

The term $W_0^{(2)\prime}[\rho]$ in Eq. (10) is determined from the contribution of the second-order correction to the correlation energy $E_{\rm c}^{(2)}$ given by Eq. (14) in Ref. [23]. Using the linear expansion $W_\alpha = W_0 + \alpha W_0^{(2)\prime}$ and performing the integral in Eq. (7) gives $W_0^{(2)\prime}[\rho] = 2\times E_{\rm c}^{(2)}$, with $E_{\rm c}^{(2)} \approx g_v \times 0.105$ Hartree. We use Hartree units throughout the paper.

The RPA density-density response function is,

$$\begin{aligned} \chi_\alpha(\boldsymbol{q},i\omega) &= \frac{\chi_0(\boldsymbol{q},i\omega)}{1-\alpha v_q\chi_0(\boldsymbol{q},i\omega)} \\ \chi_0(\boldsymbol{q},i\omega) &= g_s g_v\int d^2\boldsymbol{k}\frac{f_k - f_{\mathbf{k}+\mathbf{q}}}{\hbar\omega + \varepsilon_{\boldsymbol{k}} - \varepsilon_{\boldsymbol{k}+\boldsymbol{q}} + i\eta}. \end{aligned} \quad (12)$$

$f_{\boldsymbol{k}}$ is the Fermi-Dirac function for the wave vector $\boldsymbol{k}$, g_s and g_v are the spin and valley degeneracies, $\varepsilon_{\boldsymbol{k}}$ is the lowest energy band, and $\eta > 0$ is an infinitesimal number.

The expression for $W_0'[\rho]$ in Eq. (10) then gives

$$W_0'[\rho] = -\frac{\hbar}{2\pi\rho}\sum_{\boldsymbol{q}} v_q^2 \int_0^\infty d\omega \chi_0(\boldsymbol{q}, i\omega)^2 + 2E_c^{(2)}. \quad (13)$$

The integrals in Eqs. (10) must be obtained to an extremely high accuracy. With our approach we can arrive at the accuracy needed with computational times that are orders of magnitude less than those for the equivalent QMC calculations.

For the case of TMDs with $g_s = 2$ and $g_v = 2$ we assume a parabolic dispersion $\varepsilon_{\boldsymbol{k}} = \hbar^2 k^2/2m_e^*$. Due to the existence of the large semiconducting gap we can neglect the influence of the hole band in the response function.

Strongly-interacting regime. In the opposite limit of large $\alpha \to \infty$, the ground state is the classical WC. We can treat the classical crystal as a collection of neutral unit cells, each cell containing its electron, embedded in a uniform neutralizing background. To determine the total energy, we represent each unit cell as a disk of diameter r_0 with the electron at its center. $r_0 = 1/\sqrt{\pi\rho}$ is the average interparticle spacing. W_∞ is the electrostatic energy of a single unit cell consisting of the potential energy between the electron and the positive charged disk $E_{e\oplus}$ plus the self energy of the charged disk $E_{\oplus\oplus}$,

$$W_\infty = E_{e\oplus} + E_{\oplus\oplus} = -\frac{2}{r_s} + \frac{8}{3\pi r_s}. \quad (14)$$

Having W_0, W_0', and W_∞ we obtain the correlation energy using Eq. (9).

In Fig. 1(a) we compare our results for the correlation energy $E_c = E_{xc}[\rho] - W_0$ (red curve) with those obtained from diffusion QMC (open circles) and pure RPA (green curve) for a one-valley 2DEG system. Comparing with QMC data, adopted from Refs. [2] and [3] we see that our approach exhibits excellent agreement. We also obtained the correlation energy as a function of r_s for a monolayer TMD [Fig. 1(b)], which we compare with the corresponding QMC calculations for the two-valley 2DEG [6]. We found that the relative errors between the correlation energies of the present approach and QMC are always less than 5%.

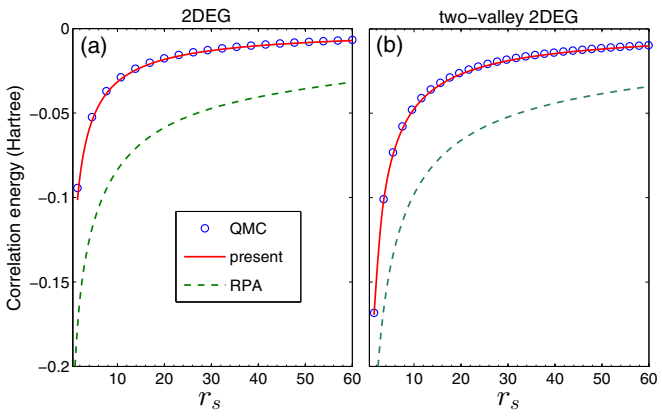

FIG. 1. Correlation energy of a uniform (a) one-valley 2DEG and (b) two-valley 2DEG systems. The results of the present approach are the solid red curves. The QMC results (blue open dots) are taken from Refs. [2] and [3] for one-valley and Ref. [6] for two-valley 2DEG systems. The pure RPA results are also shown (dashed green curves).

IV. WIGNER CRYSTALLIZATION

We obtain the total energy per particle, $\epsilon[\rho] = E/\int d^2r\rho_0$, defined in Eq. (1), for a liquid of uniform density ρ_0 and for a WC with nonuniform density distribution $\rho(\boldsymbol{r})$ given by the variational form,

$$\rho(\boldsymbol{r}) = \frac{\beta}{\pi}\sum_{m,n} \exp[-\beta(\boldsymbol{r} - m\boldsymbol{a}_1 - n\boldsymbol{a}_2)^2]\,. \quad (15)$$

$\rho(\boldsymbol{r})$ is a superposition of normalized isotropic Gaussians centered on the WC lattice sites. m and n are integers and $\boldsymbol{a}_1 = (a,0)$ and $\boldsymbol{a}_2 = (-a/2, \sqrt{3}a/2)$ are the lattice vectors for the two-dimensional hexagonal lattice. $\boldsymbol{a}_1$ and $\boldsymbol{a}_2$ are determined by the average electron density, with $a = \sqrt{2/\sqrt{3}\rho_0}$. The variational parameter β determines the degree of localization on the lattice sites. Equation (15) may also be written as a summation of the reciprocal-lattice vectors $\boldsymbol{k}_{mn}$, viz.

$$\rho(\boldsymbol{r}) = \rho_0 \sum_{m,n} e^{-k_{mn}^2/4\beta} e^{i\boldsymbol{k}_{mn}\cdot\boldsymbol{r}}. \quad (16)$$

We determine the total ground state energy $E[\rho]$ from Eqs. (1)–(3) and (9). Using this form of density Eq. (15), the Coulomb energy Eq. (3) can be solved analytically. The final expression of the Coulomb energy per particle is given by

$$\epsilon_{\rm coul} = \pi\rho_0 \sum_{k_{mn}\neq 0} \exp\left(-k_{mn}^2/2\beta\right)/k_{mn}. \quad (17)$$

We numerically calculate the total energy per particle of the ordered phase as follows. For fixed r_s, we calculate the total energy $\epsilon(\beta)$, with β as the variational parameter. We look for a minimum in $\epsilon(\beta)$ and use that as the energy for the inhomogeneous phase. If the minimum is at $\beta = 0$ the system is in the liquid state.

The calculated energies for densities ρ_0 and $\rho(\boldsymbol{r})$ are plotted as a function of r_s in Fig. 2 for the one-valley 2DEG system. We observe a stable WC at $r_s = 31$, in excellent agreement with QMC calculations. (At $r_s = 31$, there is a bifurcation, indicating a transition to the WC, i.e., the WC energy is lower than the liquid.) The upper inset in Fig. 2 shows the total energy as a function of the variational parameter β for two fixed values of r_s near the transition. For $r_s = 30$ we see that the minimum is at $\beta = 0$ (liquid phase), while at $r_s = 31$ the minimum energy occurs at a nonzero $\beta \sim 0.0012$ (WC phase). In the lower inset we show $\beta_{\rm min}$, the value of β at which the energy is minimum, as a function of r_s. Since at $r_s = 31$ the localization parameter is $\beta_{\rm min} \approx 0.00121/(a_B^*)^2$, and for the hexagonal WC lattice constant $a = \sqrt{2\pi/\sqrt{3}r_s a_B^*}$, we obtain for the half widths of the Gaussians $\sigma \approx 0.3a$, indicating localized WC density profiles around each lattice point.

The liquid and WC ground state energies for a two-valley 2DEG system corresponding to monolayer TMDs are shown in Fig. 3. We observe a transition into WC at $r_s = 30$. For the two-valley case the plot $\beta_{\rm min}$ as function of r_s is very similar to the one-valley case (lower inset in Fig. 2), and our discussion for the amount of localization remains the same.

Our result for the transition density at $r_s = 30$ in a two-valley 2DEG system is in contrast with results obtained using QMC [6]. Reference [6] reports the WC transition in the two-valley system at $r_s \approx 45$, corresponding to a much lower

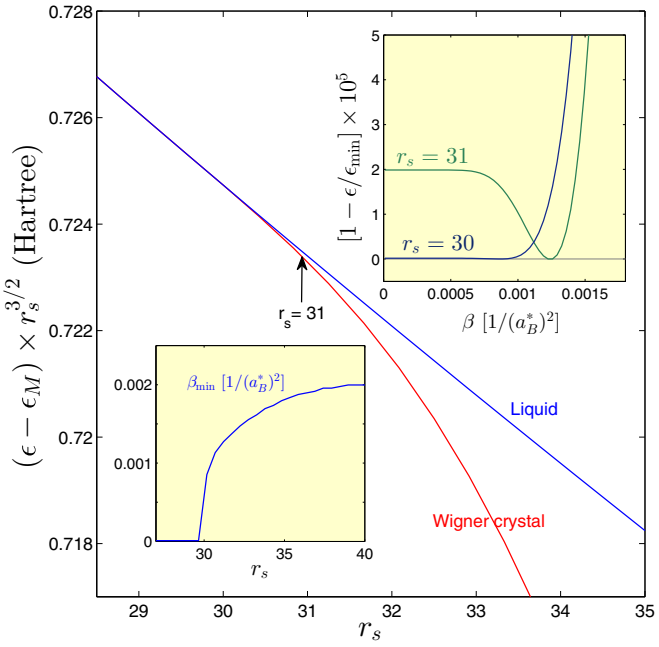

FIG. 2. The total energy per particle of a one-valley 2DEG system for the liquid (blue curve) and WC (red curve) phases. The transition to a WC occurs at $r_s \approx 31$, indicated by the vertical arrow in the figure. Upper inset: total energy as a function of variational parameter β for $r_s = 30$ (blue curve) and $r_s = 31$ (green curve). Lower inset: $\beta_{\min}$ as a function of r_s. $\epsilon_M = -1.1061/r_s$ is the Madelung energy. $\epsilon_{\min}$ is the minimum of $\epsilon(\beta)$.

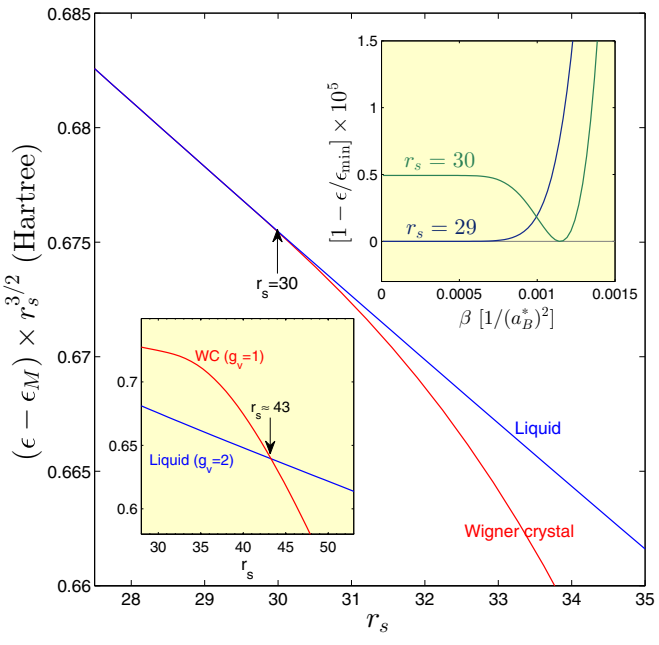

FIG. 3. The total energy per particle of a two-valley 2DEG system for the liquid (blue curve) and WC (red curve) phases. The transition to a WC occurs at $r_s = 30$, indicated by the vertical arrow in the figure. Upper inset: total energy as a function of variational parameter β for $r_s = 29$ (blue curve) and $r_s = 30$ (green curve). Lower inset: total ground state energies as function of r_s for the $g_v = 2$ liquid with a $g_v = 1$ WC (see text).

TABLE I. Wigner crystal electron density of monolayer TMDs at $r_s = 30$. The effective electron masses (m_e^*) are taken from Ref. [24] and the out-of-plane (in-plane) dielectric constants $\kappa_\perp(\kappa_\parallel)$ from Ref. [25].

TMD	MoS_2	$MoSe_2$	WS_2	WSe_2	$MoTe_2$	WTe_2
$\kappa_\perp(\kappa_\parallel)$	4.8(3.0)	6.9(3.8)	4.4(2.9)	4.5(2.9)	8(4.4)	5.7(3.3)
$m_e^*\ [m_0]$	0.46	0.56	0.26	0.28	0.62	0.26
$\rho_0\ [\times 10^{11}\ \mathrm{cm}^{-2}]$	1.85	1.5	0.66	0.875	1.37	0.45

transition density than for the one-valley 2DEG. In Ref. [6] the authors correctly note that the liquid energy reduces with the addition of a second valley because the kinetic, exchange, and correlation energies reduce. However they incorrectly assumed that the WC energy is independent of the increase in the number of components (spin and valley). In their approach, since the liquid energy is lower with two valleys while the WC energy remains unchanged, the liquid energy crosses the WC energy at a larger r_s. In the lower inset of Fig. 3 we indeed confirm that the $g_v = 1$ WC ground state energy crosses the $g_v = 2$ liquid energy at $r_s \approx 43$, which is consistent with Ref. [6].

However, the WC energy is in fact also reduced when the number of valleys is increased. This can be seen by comparing QMC results for the fully spin-polarized and unpolarized 2DEG in the WC regime. One can compare the WC energy at $\xi = 0$ (unpolarized) and $\xi = 1$ (fully-polarized) in Fig. 5 of Ref. [2]. By strict analogy, this energy difference will be the same for the unpolarized WC between the one- and two-valley systems. Thus both the liquid and the WC energy reduce when we go from the one-valley to the two-valley system. The reduction in energy turns out to be similar for the liquid and the WC, and so the WC transition density does not change very much between the one- and two-valley systems (i.e., from $r_s = 31$ to 30).

The results for the corresponding electron density at $r_s = 30$, i.e., in the WC regime, are shown in Table I for different TMDs. The electron density is calculated using $\rho_0 = 1/\pi(a_B^* r_s)^2$ where $a_B^* = \hbar^2\kappa/e^2 m_e^*$ with $\kappa = \sqrt{\kappa_\perp \kappa_\parallel}$. We find that $r_s = 30$ corresponds to carrier densities $\rho_0 \gtrsim 0.4 \times 10^{11}\ \mathrm{cm}^{-2}$ for the TMD monolayers of Table I, which is well within the lower limit of experimentally attainable densities for monolayer TMDs (of the order of $\rho \gtrsim 10^{10}\ \mathrm{cm}^{-2}$, e.g., see Refs. [26–28]).

V. CONCLUSIONS

In summary, we have presented a new approach to obtain the correlation energy in 2D systems. The approach is based on an interpolation of the exchange-correlation energy between the weakly-interacting regime and the strongly-interacting classical regime. For the weakly-interacting limit we employed RPA which is exact in this limit. In the strong interaction regime, i.e., in the low density limit, a WC occurs with the electrons forming a lattice, and we obtained the electrostatic energy for an assembly of unit cells that are neutralized by a uniformly charged background. We calculated the correlation energies for one- and two-valley 2DEG systems. The present approach is extremely fast and provides accurate results in

excellent agreement with QMC. The approach can readily be extended to: (i) 2D systems with nonparabolic low energy bands such as the bands present in few-layer graphene, and (ii) to nonzero temperatures.

We utilized density-functional theory within the local-density approximation to contrast the zero-temperature transition from a Fermi liquid to the WC phase in one- and two-valley 2DEGs. We find that the WC transition occurs for the one- and two-valley systems at very similar densities, i.e., around $r_s \sim 30$ in contrast to an earlier claim [6] that r_s should be much larger for a two-valley system. In the two-valley monolayer TMDs, $r_s = 30$ corresponds to a density $\rho_0 \gtrsim 0.4 \times 10^{11}$ cm^{-2}, which lies well within the experimentally achievable density range. We conclude that monolayer TMDs could be ideal systems for the observation of WC in zero magnetic field.

The results in this paper are for zero temperature. However, the energy differences in the total energies of the Fermi liquid and the WC phase could provide us with an upper limit estimate of the transition temperatures. We found this energy difference of the order of 10 K at $r_s \approx 30$.

There are number a of ways that a WC phase could be experimentally identified. Wigner crystallization is accompanied by a transition to an insulating state caused by pinning of the Wigner lattices by residual disorder. This can be detected using transport measurements [29,30]. A modulated density distribution can be experimentally observed using scanning tunneling microscopy (STM). This, for example, has been used to identify a charge-density-wave phase [31,32] and could be equally well used to observe a WC phase.

ACKNOWLEDGMENTS

This work was partially supported by the Flanders Research Foundation (FWO) and the Methusalem program of the Flemish government. D.N. acknowledges support by the University of Camerino FAR project CESEMN.

[1] E. Wigner, Phys. Rev. **46**, 1002 (1934).
[2] B. Tanatar and D. M. Ceperley, Phys. Rev. B **39**, 5005 (1989).
[3] C. Attaccalite, S. Moroni, P. Gori-Giorgi, and G. B. Bachelet, Phys. Rev. Lett. **88**, 256601 (2002).
[4] F. Rapisarda and G. Senatore, Austr. J. Phys. **49**, 161 (1996).
[5] N. D. Drummond and R. J. Needs, Phys. Rev. Lett. **102**, 126402 (2009).
[6] M. Marchi, S. De Palo, S. Moroni, and G. Senatore, Phys. Rev. B **80**, 035103 (2009).
[7] A. H. Castro Neto, F. Guinea, N. M. R. Press, K. S. Novoselov, and A. K. Geim, Rev. Mod. Phys. **81**, 109 (2009).
[8] M. Chhowalla, Zh. Liu, and H. Zhang, Chem. Soc. Rev. **44**, 2584 (2015).
[9] Sh. Z. Butler, Sh. M. Hollen, L. Cao, Y. Cui, J. A. Gupta, H. R. Gutièrrez, T. F. Heinz, S. S. Hong, J. Huang, A. F. Ismach, E. J-. Halperin, M. Kuno, V. V. Plashnitsa, R. D. Robinson, R. S. Ruoff, S. Salahuddin, J. Shan, L. Shi, M. G. Spencer, M. Terrones, W. Windl, and J. E. Goldberger, ACS Nano **7**, 2898 (2013).
[10] S. Das Sarma, Sh. Adam, E. H. Hwang, and E. Rossi, Rev. Mod. Phys. **83**, 407 (2011).
[11] H. P. Dahal, Y. N. Joglekar, K. S. Bedell, and A. V. Balatsky, Phys. Rev. B **74**, 233405 (2006).
[12] K. F. Mak, K. He, C. Lee, G. H. Lee, J. Hone, T. F. Heinz, and J. Shan, Nat. Mater. **12**, 207 (2013).
[13] S. Larentis, J. R. Tolsma, B. Fallahazad, D. C. Dillen, K. Kim, A. H. MacDonald, and E. Tutuc, Nano Lett. **14**, 2039 (2014).
[14] Z. Y. Zhu, Y. C. Cheng, and U. Schwingenschlögl, Phys. Rev. B **84**, 153402 (2011)
[15] R. G. Parr and W. Yang, *Density-Functional Theory of Atoms and Molecules* (Oxford University Press, New York, 1989); R. M. Dreizler and E. K. U. Gross, *Density Functional Theory* (Springer, Berlin, 1990).
[16] P. Gori-Giorgi, M. Seidl, and G. Vignale, Phys. Rev. Lett. **103**, 166402 (2009).
[17] R. Q. Hood, M. Y. Chou, A. J. Williamson, G. Rajagopal, R. J. Needs, and W. M. C. Foulkes, Phys. Rev. Lett. **78**, 3350 (1997); M. Levy and J. P. Perdew, Phys. Rev. A **32**, 2010 (1985).
[18] M. Seidl, Phys. Rev. A **60**, 4387 (1999).
[19] M. Seidl, J. P. Perdew, and M. Levy, Phys. Rev. A **59**, 51 (1999).
[20] M. Seidl and J. P. Perdew, Phys. Rev. B **50**, 5744 (1994).
[21] A. Görling and M. Levy, Phys. Rev. B **47**, 13105 (1993).
[22] G. Giuliani and G. Vignale, *Quantum Theory of the Electron Liquid* (Cambridge University Press, New York, 2008).
[23] A. K. Rajagopal and J. C. Kimball, Phys. Rev. B **15**, 2819 (1977).
[24] A. Kormányos, G. Burkard, M. Gmitra, J. Fabian, V. Zólyomi, N. D. Drummond, and V. Fal'ko, 2D Mater. **2**, 049501 (2015).
[25] A. Kumar and P. K. Ahluwalia, Physica B: Condensed Matter **407**, 4627 (2012).
[26] K. F. Mak, K. He, J. Shan, and T. F. Heinz, Nat. Nanotechnol. **7**, 494 (2012); J. S. Ross, S. Wu, H. Yu, N. J. Ghimire, A. M. Jones, G. Aivazian, J. Yan, D. G. Mandrus, Di Xiao, W. Yao, and X. Xu, Nat. Commun. **4**, 1474 (2013).
[27] K. F. Mak, K. L. McGill, J. Park, and P. L. McEuen, Science **344**, 1489 (2014).
[28] S. B. Desai, S. R. Madhvapathy, A. B. Sachid, J. P. Llinas, Q. Wang, G. H. Ahn, G. Pitner, M. J. Kim, J. Bokor, Ch. Hu, H.-S. Ph. Wong, and A. Javey, Science **354**, 99 (2016).
[29] V. J. Goldman, M. Santos, M. Shayegan, and J. E. Cunningham, Phys. Rev. Lett. **65**, 2189 (1990).
[30] F. I. B. Williams, P. A. Wright, R. G. Clark, E. Y. Andrei, G. Deville, D. C. Glattli, O. Probst, B. Etienne, C. Dorin, C. T. Foxon, and J. J. Harris, Phys. Rev. Lett. **66**, 3285 (1991).
[31] R. V. Coleman, B. Giambattista, P. K. Hansma, A. Johnson, W. W. McNairy, and C. G. Slough, Adv. Phys. **37**, 559 (1988).
[32] Ch. Brun, Zh.-Zh. Wang, P. Monceau, and S. Brazovskii, Phys. Rev. Lett. **104**, 256403 (2010).